Clay mineral evidence of nepheloid layer contributions to the Heinrich layers in the northwest Atlantic

Viviane Bout-roumazeilles, Elsa Cortijo, Laurent Labeyrie, Pierre Debrabant

Clay mineral evidence of nepheloid layer contributions to the Heinrich layers in the northwest Atlantic

Viviane Bout-Roumazeilles [a,*], Elsa Cortijo [b], Laurent Labeyrie [b,c], Pierre Debrabant [d]

a Faculteit der Aardwetenschappen, Vrije Universiteit Amsterdam, De Boelelaan 1085, 1081 HV Amsterdam, The Netherlands

* Corresponding author.

b Centre des Faibles Radioactivités, laboratoire mixte CNRS-CEA, 91 198 Gif-sur-Yvette, France

c Département des Sciences de la Terre, bât. 504, Université de Paris Sud, 91 045 Orsay, France

d Laboratoire de Sédimentologie et Géodynamique, URA 719 CNRS, Université de Lille 1, 59 655 Villeneuve d'Ascq, France

Keywords: North Atlantic; clay minerals; nepheloid layer; Pleistocene

Abstract

The clay fraction of four cores drilled in the north Atlantic Ocean was studied at a very high resolution over the last 150 ka in order to record the mineralogical signature of Heinrich events. Factor analysis of clay mineralogy establishes that three independent factors represent the main variations: a 'detrital factor' (illite C chlorite C kaolinite), a 'smectite factor', and a 'mixed-layer factor' (IVML: illite-vermiculite mixed-layered clay). The clay mineral fraction of core SU90-38 drilled in the northeastern Atlantic basin did not record any Heinrich event, whereas large changes in the clay mineral fraction occurred during Heinrich events H1, H2, H4, and H5 in the three cores from the northwestern Atlantic basin (cores SU90-08, SU90-11, and SU90-12). Heinrich layers are characterized by increases in the detrital factor in cores SU90-08 and SU90-11, and sharp increases in the mixed-layer factor in cores SU90-11 and SU90-12. The geographical setting of the cores, the pattern of surface, intermediate and deep water circulation, and the main sources of clay minerals allow recognition of two major mechanisms involved in the deposition of the Heinrich Layers: (1) an increased supply of detrital clay minerals by the icebergs; and (2) a specific input of illite-vermiculite mixed-layer clay minerals by a nepheloid layer.

1. Introduction

High-resolution palaeoceanographic studies in the North Atlantic Ocean provide much evidence of massive fluxes of coarse detrital material that are interpreted as a consequence of abrupt climatic changes. The Heinrich layers corresponds to short periods of very high sedimentation rates These 'Heinrich layers' mainly occur within a preferential accumulation belt, between 40 and 50ºN, along the edge of the polar front (Ruddiman, 1977; Heinrich, 1988; Bond et al., 1992; Broecker et al., 1992; Grousset et al., 1993). These events are also characterized by decreases in the number of species and abundance of foraminifers, the resulting assemblages being dominated by the cold species *N. pachyderma* (left coiling) (Bond et al., 1992). A high content of detrital carbonate, especially dolomite, suggests that most of the terrigenous material originates from the eastern margin of the Laurentide ice-sheet (Andrews and Tedesco, 1992; Huon and Ruch, 1992; Andrews et al., 1994). Heinrich events are generally closely associated with instabilities of the Laurentide ice-sheet. MacAyeal (1993) suggested that the Heinrich events were caused by free oscillations of the Laurentide ice-sheet: when the frozen sediments, at the base of the ice-sheet, started to thaw, they formed a lubricant and the ice-sheet began to slip. Ice flow from Hudson Bay may have delivered coarse particles (between 150 μm and several millimetres), eroded from the calcareous Paleozoic bedrock, to the continental slope and to the deep oceanic basin. Debris flows, turbidity currents, and intermediate water masses may also be involved in producing the Heinrich layers. This is evident from the high accumulation rates observed in sediments sampled outside the main icebergs pathways (Andrews and Tedesco, 1992). Here we used clay particles (<2 μm) which are easily transported by oceanic currents, to demonstrate the contribution of a nepheloid layer to the Heinrich layer deposits in the northwestern Atlantic basin.

2. Material and methods

2.1. Core settings

Four sediment cores from the cruise Paleocinat I in 1990 were studied: SU90-08, SU90-11, SU90-12, and SU90-38 (Table 1; Fig. 1). Three cores were taken from the northwestern Atlantic basin: the southernmost core SU90-08 is located at 43ºN near the Azores, on the western flank of the mid-oceanic ridge at 3080 m depth, in a quiet deep environment; core SU90-11 (3645 m) and SU90-12 (2950 m) are situated on seamounts at 44 and 51ºN, respectively, near the entrance of the Labrador Sea. Cores SU90-11 and SU90-12

are situated on seamounts at 1000 m above the sea-floor: sedimentation at these sites is therefore only controlled by intermediate or/and surface water masses flowing out the Labrador sea. Core SU90-38 was sampled in the northeastern Atlantic basin, at 54ºN, near Rockall Plateau, at 2900-m water depth. This site is under the influence of the eastern drift of the North Atlantic Deep Water overflowing the Wyville–Thomson rise, and by surface water masses originating from the Greenland and Norwegian seas.

2.2. Correlation and chronology

The age model for each site is based on a comparison between the benthic and/or planktonic $\delta^{18}O$ records and the spectral mapping SPECMAP stack (Martinson et al., 1987) using the Analyseries software (Paillard et al., 1996). A linear interpolation was applied between the stratigraphic levels identified (Table 2), assuming that the sedimentation rate was constant between these levels. The age–depth relations are given in Table 2 and shown in Fig. 2. The oxygen isotope analysis of foraminifers was measured on an automatic carbonate preparation line coupled to a Finnigan MAT 251 mass spectrometer (Centre des Faibles Radioactivités, Gif-sur-Yvette, France) Isotopic stages and their boundaries were deduced from isotopic curves, magnetic susceptibility, and reflectance (Grousset et al., 1993; Cortijo et al., 1995). The mean sedimentation rate of core SU90-08 is about 4.2 cm/ka^{-1} and varies along the series (Fig. 2). The sedimentation rate is higher in the upper part of the core (0–107.6 ka), 5.3 cm/ ka^{-1}, and between 183.4 and 225.2 ka, where it reaches 6.2 cm/ ka^{-1}. Core SU90-11 records slower sedimentation rates than core SU90-08: the mean value is of 2.9 cm/ ka^{-1} (Fig. 3). The highest rates in this core are observed in the upper part (0–122.2 ka), 3.8 cm/ ka^{-1}. Core SU90-12 has the slowest and most regular sedimentation rate, with a mean value of 2.9 cm/ ka^{-1} (Fig. 3). The mean ages (Fig. 2) for the Heinrich layers (14.5 ka for H1, 22 ka for H2, 27 ka for H3, 40 ka for H4, 50 ka for H5, and 60 ka for H6) are deduced from the age model for core SU90-08 (Grousset et al., 1993).

2.3. Method of clay analysis

All samples were first decalcified with 0.2 *N* hydrochloric acid. The excess acid was removed by repeated centrifugations. The clay-sized fraction (<2 μm) was isolated by settling, and oriented on glass slides (oriented mounts). Three XRD (X-ray diffraction) determinations were performed: (a) untreated sample; (b) glycolated sample (after saturation for 12 h in ethylene glycol); and (c) sample heated at 490ºC for two hours (Holtzapffel, 1985). The analyses were run on a Philips PW 1710 X-ray diffractometer, between 2.49 and 32.5º2θ.

Each clay mineral is then characterized by its layer plus interlayer interval as revealed by XRD analysis. Smectite is characterized by a peak at 14 Å on the untreated sample test, which expands to 17 Å after saturation in ethylene-glycol and retracts to 10 Å after heating. Illite presents a basal peak at 10 Å on the three tests (natural, glycolated, and heated). The IVML (illite-vermiculite mixed-layered clay) is determined by a peak at 12 Å which does not expand after saturation in ethylene-glycol and retracts to 10 A° after heating. Chlorite is characterized by peaks at 14, 7, 4.72, and 3.53 Å on the three tests. Kaolinite is characterized by peaks at 7 and 3.57 Å on the untreated sample and after saturation in ethylene glycol. Both peaks disappear or are strongly reduced after heating. Semi-quantitative estimation of clay minerals abundances has been done according to the method detailed in Holtzapffel (1985).

The reproducibility of technical works and measurements was tested: 5 oriented mounts prepared from the same samples were submitted 3 times to XRD. The relative error is ±5%.

2.4. Method of factor analysis

Factor analysis has been performed on all clay abundance data. The method used the Principal Component Analysis (PCA) by the orthogonal transformation method (Johnson and Wichern, 1982; Albarède, 1995). The PCA explains the covariance structure of multivariate data through a reduction of the whole data to a smaller number of independent variables, called factors.

3. Results

3.1. General data and clay mineralogy

3.1.1. Core SU90-08

Sediments of core SU90-08 are mainly composed of gray to dark gray carbonate (foraminifera and nannofossil) oozes and muds interbedded with terrigenous muddy clay, silty mud and terrigenous mud (sand, silt and clay-sized particles mixed together). The clay mineral association is mainly composed of illite (37 7%) and smectite (33 ± 11%). Chlorite and kaolinite are less abundant with respectively 14% (±3%) and 11% (±3%) of the clay mineral association (Table 3). The random IVML constitutes less than 5% of clay minerals association (Bout- Roumazeilles, 1995). The Heinrich layers, which are characterized by their high coarse-size detrital content (calcite, dolomite, quartz, feldspars and amphiboles) are

significantly enriched in illite (Table 4), which reaches 55% of the clay mineral association. The content of chlorite (20%) and kaolinite (15%) also increases in these layers, whereas smectite sharply decreases (10%).

3.1.2. Core SU90-11

Sediments of core SU90-11 are composed of dark gray terrigenous muds interbedded with gray carbonate (nannofossils with foraminifera) muds. The clay mineral association is dominated by illite (average value of 34 ± 4%), with 17% (±7%) IVML and 20% (±4%) chlorite. Smectite and kaolinite represent 16% (±7%) and 12% (±2%) of the clay mineral association, respectively (Table 3). The Heinrich layers are characterized by high magnetic susceptibility, high detrital carbonate content, by a strong increase in IVML in the clay-size fraction, which reach 28% of the clay mineral association and absence of smectite. The percentages of chlorite and kaolinite remain stable.

3.1.3. Core SU90-12

The sediments of core SU90-12 are mainly composed of dark gray terrigenous muds, interbedded with minor levels of carbonate (nannofossils with foraminifera) muds. On the average, the clay fraction is dominated by mean values of 34% (±5%) illite and 21% (4%) chlorite (Table 3). The IVML represents 18% (±8%) of the clay mineral association. Smectite (15 ± 8%) and kaolinite (12 ± 2%) are less abundant (Bout-Roumazeilles, 1995). The Heinrich layers are characterized by high contents of IVML, which reach 32% of the clay mineral association and by low contents of smectite (8%). The content of illite, chlorite, and kaolinite slightly decreases within the Heinrich layers.

3.1.4. Core SU90-38

Core SU90-38 is composed of dark gray terrigenous muddy clay, of gray carbonate mud, and of carbonate (foraminifera with nannofossils) oozes interbedded with minor beds of silt and fine sand. The clay mineral association mostly includes illite (39±7%) and smectite (35±11%). Chlorite (14±3%) and kaolinite (12±2%) are less abundant whereas the random illite-smectite mixed-layer minerals occur as trace amounts (Table 3). No significant modification of the clay association is observed in the Heinrich layers (Heinrich layers have been distinguished on the basis of their high detrital content). Illite (42 ± 5%) and smectite (32 ± 4%) still constitute the main part of the clay mineral association, and chlorite (14±2%) and kaolinite (12 ± 3%) are less abundant.

In summary, the mean percentages of illite, chlorite, and kaolinite are essentially constant in the four cores. Illite, chlorite, and kaolinite represent 62% (core SU90-08) to 67% (core SU90-12) of the clay mineral association. Abundant IVML characterizes the clay mineral association of the western cores SU90-11 (17%) and SU90-12 (18%), whereas it is absent from the two other cores. Low abundances of smectite characterized western cores SU90-11 and SU90-12 where it constitutes only 15% of the clay mineral association. In contrast smectite constitutes more than 30% of the clay mineral fraction in cores SU90-08 and SU90-38. In core SU90-08, the Heinrich layers are characterized by high contents of illite, chlorite, and kaolinite (up to 90% of the clay mineral association), whereas smectite strongly decreases. In cores SU90-11 and SU90-12, abundant IVML (up to 32%) characterizes the Heinrich layers. Smectite disappears in the Heinrich layers of core SU90-11, and is strongly reduced in core SU90-12. There is no coherent variation of illite, chlorite, and kaolinite within the Heinrich layers: illite, chlorite, and kaolinite increase in core SU90-11, decrease in core SU90-12, and strongly increase in core SU90-08. In core SU90-38, the clay mineralogy of the Heinrich layers is not different from the rest of the core.

3.2. Results of the correlation matrix

3.2.1. Core SU90-08

The correlation matrix of core SU90-08 (Table 5) indicates that the variations in chlorite, illite, and kaolinite abundances are very well correlated ($0.7 < r < 0.8$). Smectite abundances appear to be independent of the other minerals. The principal component analysis reveals that two factors represent the major variations (0.9<factor scores<1) in all four clay minerals (Table 6). One factor (the 'ICK factor') groups together illite, chlorite, and kaolinite, whereas the other one corresponds to smectite ('smectite factor'). The primary intercorrelation indicates that the two factors ($r = 0$) are independent.

3.2.2. Core SU90-11

In core SU90-11, the variations of chlorite, illite, and kaolinite are well correlated ($r = 0.8$). They are grouped (Table 6) together in the 'detrital factor' (factor scores = 0.9). The correlation matrix (Table 5) indicates that smectite and IVML are slightly anticorrelated ($r = 0.6$). Consequently, the primary intercorrelation reveals that the 'detrital factor' is not linked with the two others, whereas the 'smectite factor' and the 'mixed-layer factor' are not totally independent ($r = 0.4$).

204

205 *3.2.3. Core SU90-12*

206 The results of the factor analysis of core SU90-12 are approximately similar to those
207 of core SU90-08. Once again, the variations of chlorite, of illite, and of kaolinite are well
208 correlated and are represented by the 'detrital factor' (Tables 5 and 6). The correlation
209 indexes between smectite and the other mineral are higher than in the cores SU90-08 and
210 SU90-11, but still below the confidence level. As a result, the intercorrelation reveals that the
211 factors are not strictly independent even if the intercorrelation index remains below the
212 confidence level ($-0.5 < r < 0.5$).

213

214 *3.2.4. Core SU90-38*

215 Correlation between the variations of chlorite, illite, and kaolinite for core SU90-38 is
216 very high ($0.8 < r < 0.9$). The variations in smectite are not significantly correlated with those
217 of the other clay minerals (Table 5). The 'detrital factor' represents the main variations of
218 illite, of chlorite, and of kaolinite (factor scores = 0.9) and the 'smectite factor' represents the
219 variations of smectite (factor score = 1).

220 Overall, the variations of illite, chlorite, and kaolinite in all the cores studied are
221 represented by the 'detrital factor'. The variations in smectite are represented by the 'smectite
222 factor' and these of the IVML by the 'mixed-layer factor'. Below we will discuss the
223 variations of each factor before, during, and after the Heinrich events H1 to H6.

224

225 *3.3. Results of the factor analysis*

226

227 *3.3.1. Core SU90-08*

228 The 'detrital factor' is low from 130 to 70 ka and shows little variations except during
229 the Heinrich events (Fig. 4). It increases very slightly during H6 and H3, whereas it increases
230 sharply and reaches its maximum values during H5, H4, H2, and H1. The 'smectite factor'
231 varies a lot during the last 130 ka. Its variations during all Heinrich events are not similar: in
232 H6 and H3, the smectite factor increases, whereas it slightly decreases in H5, H4, H2, and H1.

233

234 *3.3.2. Core SU90-11*

235 The 'detrital factor' remains stable and low between 130 and 70 ka. An increase in the
236 factor characterizes H5, H4, H2, and H1, whereas the factor does not change during H6 and
237 H3 (Fig. 5). After H5, H4, H2, and H1, it returns to its mean level. There is no coherent

variation of the ‘smectite factor’ during the Heinrich events. It remains stable during H6, H5, H3, and H2, increases in H1, and decreases in H4. The ‘mixed-layer ’ factor remains stable from 130 to 70 ka, and during H6 and H3, but shows very short increases during H5, H4, H2, and H1.

3.3.3. Core SU90-12

Major variations of the ‘detrital factor’ occur between 130 and 70 ka, whereas it remains relatively stable between 35 and 0 ka (Fig. 5). Heinrich events H6, H5, and H4 are characterized by increases of this factor, the most important variations being found in H5 and H4. Between 130 and 70 ka, the ‘smectite factor’ shows marked variations. Over the past 70 ka this factor is mostly characterized by decreases during H5, H4, and H2. The variations of the ‘mixed layer factor’ are similar to those of core SU90-11: the mixed-layer factor increases abruptly at the beginning of each Heinrich event, and then drops to below average values. This is especially obvious for H5 and H4.

3.3.4. Core SU90-38

The ‘detrital factor’ is significantly lower between 130 and 70 ka than between 70 and 10 ka. It remains stable in the upper part of the core even during Heinrich events. The ‘smectite factor’ records more variations than the ‘detrital factor’, but they are not correlated with Heinrich events: the factor decreases during H6, increases slightly during H5, H4, and H2, whereas it does not vary during H1 (Fig. 4).

In summary, the Heinrich events are not characterized by any significant variations of the ‘detrital factor’ and ‘smectite factor’ in core SU90-38, located in the northeastern Atlantic basin. By contrast, some of the Heinrich events — H5, H4, H2, and H1 — are characterized by the increase of the ‘detrital factor’ in cores SU90-08, SU90-11 and SU90-12, which were taken from the northwestern Atlantic basin. The variations of the ‘detrital factor’ associated with the Heinrich events are better developed in the southernmost cores SU90-08 (43ºN) and SU90-11 (44ºN), than in the northernmost core SU90-12 (51ºN). The ‘smectite factor’ does not show a consistent pattern of variations. In core SU90-08, the ‘smectite factor’ decreases during the Heinrich events H5, H4, H2, and H1. In the other cores, the variations of the ‘smectite factor’ are not the same during all Heinrich events. Variations in the ‘mixed-layer factor’ characterize only the westernmost cores SU90-11 and SU90-12. Sharp increases to maximum value are followed by rapid drops below average values in the Heinrich events H5,

H4, H2, and H1. In core SU90-12, the decrease of the 'mixed-layer factor ' is more drastic for H5 and H4.

4. Discussion

4.1. Clay mineral sources

Under present climatic conditions, the typical terrigenous clay minerals, illite and chlorite, mainly results from physical weathering of continental substrates at high latitudes (Biscaye, 1965; Griffin et al., 1968; Rateev et al., 1969; Millot, 1970; Lisitzin, 1972; Chamley, 1975; Chamley, 1989). During glacial times or when climatic conditions were colder, physical weathering was intensified, leading to greater rock fragmentation and disintegration, and therefore increasing the terrigenous input to the ocean (Chamley, 1989). In the northeastern Atlantic basin, the main sources of chlorite and illite are the Scandinavian shields, Scotland, Ireland and Greenland (Moyes et al., 1964; Biscaye, 1965; Griffin et al., 1968). In the northwestern Atlantic basin, chlorite and illite derive from the Precambrian and Paleozoic igneous and sedimentary rocks of the North American continent, Baffin Island, and Greenland (Piper and Slatt, 1977; Petersen and Rasmussen, 1980; Thiébault et al., 1989).

Kaolinite, in the northernmost Atlantic basin, is essentially inherited from adjacent land masses where it formed during pre-glacial times and is derived from pre-existing paleosols, sediments or sedimentary rocks on the continents (Darby, 1975; Naidu et al., 1982; Sancetta et al., 1985; Chamley, 1989; Thiébault et al., 1989). In the northeastern Atlantic basin, the sources of kaolinite are the Mesozoic areas around the Barents Sea (Kuhlemann et al., 1993) and southeastern Svalbard (Elverhøi, 1979). In the northwestern Atlantic basin, kaolinite could derive from sedimentary formations of the North American continent (Boyd and Piper, 1976; Piper and Slatt, 1977) such as the black Cretaceous mudstones of Labrador (Jennings, 1993).

The IVMLs are not commonly observed in sediments, and constitute a good discriminant for particle sources. They mainly result from moderate pedogenic processes during interglacial Quaternary conditions at mid- to high latitudes. They seem to result especially from the weathering of mica in an alkaline environment (Millot, 1970) or from pedogenic transformation in soils under temperate climatic conditions (Berry and Johns, 1966). IVML main sources are from Tertiary sediments in Virginia (McCartan, 1988), the Canadian Appalachians Mountains (Yang and Hesse, 1991) and in the Adirondack Mountains, NY State (April et al., 1986). IVMLs form from pedogenic processes in the

Canadian Appalachians Mountains and are transported by run-off to the Labrador shelf area. IVML has been also identified as reworked material in fluvial sediments on the western coast of Greenland (Petersen and Rasmussen, 1980). Recent work (Fagel et al., 1996) in the Labrador basin demonstrates that IVMLs are abundant at shallow depth in Labrador shelf sediments (<300 m water depth). But their abundance decreases to traces at greater water depth and they have not been found yet in the deepest parts of the Labrador basin. At 2698 m off New Jersey (ODP Site 905A) IVML constitute 5–25% of the clay mineral association of Pleistocene sediments (Deconinck and Vanderaveroet, 1996). IVMLs are assumed to be inherited from ancient soils developed on nearby mica-rich schists (Rich, 1956).

Smectite is common in North Atlantic sediments. It results from the chemical alteration of basalts, volcanic ashes and glasses, from pedogenic evolution of illite, or from erosion of old sediments formed during intervals when local climatic conditions (warm and hydrolyzing) allow pedogenic formation of smectite (Desprairies and Bonnot-Courtois, 1980; Chamley, 1989). Iceland, the Faeroe Islands (Parra et al., 1985), and the North European continental Tertiary formations, constitute the main sources of smectite in the northeastern Atlantic basin. Smectite is less abundant in the northwestern Atlantic basin, because of greater distance from the main continental sources (Berthois et al., 1973; Grousset, 1983; Grousset and Chesselet, 1986), or because climatic conditions in adjacent continental areas were too cold to allow pedogenic formation of smectite during the Quaternary. Nevertheless, smectite represents 5–50% of the clay mineral association in the Labrador Sea (Nielsen et al., 1989; Thiébault et al., 1989; Fagel et al., 1996). The main sources of smectite in this area are the northeastern Canadian Tertiary formations and smectite is also a main component in sediments off Cumberland Sound and Baffin Island (Jennings, 1993; Andrews et al., 1996; Jennings et al., 1996). Higher abundances of smectite at the rise/slope boundary on the path of the Western Boundary Under-Current could result from the mixture of particles transported from the Northern Labrador Sea and from the Iceland–Reykjanes ridge (Fagel et al., 1996).

4.2. Dynamics of the Heinrich events

Clay minerals allow recognition of temporal variations in the characteristics of the Heinrich events in the following ways:

– In the northeastern Atlantic basin, Heinrich layers, which are otherwise characterized by an increased coarse fraction, are not characterized by any variation of the clay mineral association. By contrast, in the northwestern Atlantic basin, most of the

Heinrich layers are also characterized by important modifications in the clay mineral associations.

- The Heinrich layers of the North West Atlantic are enriched in 'detrital' clay minerals (i.e. illite C chlorite C kaolinite) especially in the southern cores SU90-08 (43ºN) and SU90-11 (44ºN). However, the more recent Heinrich layers (H1 and H2) of the northernmost core SU90-12 do not show any enrichment in detrital clay minerals.
- Increased supply of detrital clay minerals is especially obvious in H1 (14.5 ka), H2 (22 ka), H4 (40 ka), and H5 (50 ka). Only slight increases are observed in H3 (27 ka) and H6 (60 ka) (the 'detrital factor' slightly increases).

Since illite, chlorite, and kaolinite all increase simultaneously during the Heinrich events, their input probably result from the same mechanism. This mechanism starts abruptly as shown by the rapid increase of the 'detrital factor' at the beginning of the Heinrich events. Chlorite, illite, and kaolinite, in the northwestern Atlantic basin, derive from the erosion of Precambrian/Paleozoic igneous rocks (Piper and Slatt, 1977; Thiébault et al., 1989) and Paleozoic/Cretaceous sedimentary rocks of the north American continent, especially in the Labrador and Baffin Bay area (Boyd and Piper, 1976; Jennings, 1993). According to the main actual surface-water circulation pattern in the western basin (Fig. 1), an ice-rafting mechanism is then assumed to be responsible for the enhanced supply of detrital clay minerals as for detrital carbonates (Andrews and Tedesco, 1992; Bond et al., 1992; Grousset et al., 1993). A logical model is as follows: during the growth of the Laurentide ice-sheet, its base eroded the sedimentary formations and bedrock of the Canadian Shield, and consequently glacially reworked detrital carbonates (calcite and dolomite) and detrital clay minerals were transported into the ice to the shelf area. There, fragmentation of the ice-sheet released icebergs containing detrital clay minerals, which followed the main surface circulation pattern (Labrador Current) to the North Atlantic ocean (Fig. 1). During their southern transfer, the icebergs began to melt and progressively discharged their detrital load. The northernmost cores (SU90-11 and SU90-12) are located on seamounts, 1000 m above the sea floor, so bottom currents cannot be involved in particle transport to these sites. Close association of increased detrital clays with sand-sized ice-rafted particles at site SU90-11 suggest that sedimentation processes involved ice melting. Melting accelerated when icebergs reached warmer waters near the polar front, and changed direction to follow the North Atlantic Drift, increasing the incorporation of ice-rafted particles (including detrital clays) to the sediment.

The Heinrich events are also characterized by:

- An increased supply of IVML supply in (39ºW), whereas IVMLs are absent from the eastern Atlantic basin and in the eastern part of the northwestern Atlantic basin (core SU90-08, 30ºW). The comparison between the variations of both 'detrital' and 'mixed-layer' factors in cores SU90-11 and SU90-12 indicates that increased supply of mixed-layer supply precedes deposition of typically detrital clay minerals. Moreover, IVML supply stops before detrital clays began to decrease. It suggests (1) that two different mechanisms are involved, and (2) that the IVML supply results from a mechanism more rapid than those responsible for the supply of illite, chlorite, and kaolinite.
- Increased supply of IVML also occurs in the two more recent Heinrich events (H1 and H2) of core SU90-12 where there is no evidence of any increased detrital ice-rafted clays.

All this evidence indicates that IVMLs have not been transported by ice like detrital carbonates and detrital clay minerals. Moreover, the specific location of the cores SU90-11 and SU90-12 (on seamounts, 1000 m above the sea floor) prevents particle transport to these sites by bottom currents. These minerals may be carried either by deep to intermediate water masses or by eolian circulation. Comparison of the distribution of the IVML in the northwestern Atlantic basin and of the main atmospheric circulation pattern is not consistent with an eolian supply (Bout-Roumazeilles, 1995). Therefore, intermediate to deep water-circulation may be responsible for the supply of the mixed-layer clays during the Heinrich events. This supply could be associated to the mechanism of the Labrador nepheloid layer (Eittreim et al., 1969; Eittreim and Ewing, 1974; Biscaye and Eittreim, 1974, 1977) or to ice-shelf flow (Hulbe, 1997). Ice-flow during fragmentation of ice caps and release of icebergs eroded surface sediments of the continental shelves. In the Labrador Sea, these shallow sediments are enriched in IVML (Bout-Roumazeilles, 1995; Fagel et al., 1996), formed through pedogenic processes and transported to the shelf area by run-off during interglacials (Fig. 7). These particles contribute to the formation of a nepheloid layer which flows at intermediate depth because of relatively high density. Increased fragmentation of the Labrador ice sheet during some Heinrich events (H1, H2, H4 and H5) may have resulted in intensified erosion of IVML-rich surface sediments on the shelf. Increased IVML appears directly linked to ice-sheet dynamics. Increases of both ice-rafted detritus and IVML characterizes the Heinrich events but they are not closely dependent (Fig. 6). This suggests variations of ice-sheet dynamics in relation to climate, which need further investigations.

404

405 *4.3. Spatial distribution of the nepheloid layer*

406 Extension of the nepheloid layer can be estimated by comparison of mineralogical
407 data from subsurface sediments at various depths, latitudes and longitudes of the northwestern
408 Atlantic (Table 7). The database includes the Paleocinat I cruise mineralogical data (Bout-
409 Roumazeilles, 1995), and mineralogical results (Fagel et al., 1996) from the Labrador Sea and
410 the North Atlantic Ocean (cruises Hudson 90 and 91).

411 The IVMLs are abundant at shallow water depth (301 to 530 m) of the southern
412 Labrador shelf (cores 1, 2, and 3, Table 7). They decrease at deeper water depth: 5% in core 4
413 (1364 m), trace amounts in cores 5 (1984 m) and 6 (2648 m). These results indicate that the
414 nepheloid layer formed in shallow areas, especially off southern Labrador. The presence of
415 IVML in subsurface sediments from seamounts east of the shelf (cores 90-13 and SU90-12)
416 provides evidence of the main southeastward direction of the nepheloid layer (Fig. 7).
417 However, it is surprising not to find IVML in core 7 nor in cores 25, 27, and 28 (Fagel et al.,
418 1996). This could result from the deep location of these cores (between 3378 and 3992 mbsf),
419 but in this case it is difficult to explain the presence of IVML in core SU90-11 (3645 mbsf).
420 Nevertheless the northern edge of the nepheloid layer is roughly situated near 57ºN. This edge
421 is related to the position of the intermediate- to deep-water current, which flows from the
422 Irminger basin to the Labrador basin off southern Greenland. IVMLs have not been reported
423 from the northeastern Atlantic basin. The analysis of the clay mineral fraction from cores
424 9003, 9005, 9006, 9009, 9010, and SU90-08 does not reveal any traces of IVML in
425 subsurface sediments. This indicates that the eastern edge of the nepheloid layer (Fig. 7) is
426 situated somewhere between 39ºW (core SU90-12) and 34ºW (core 9010). Hence it appears
427 that the mid-oceanic ridge acts as a barrier to prevent the extension of the nepheloid layer into
428 the northeastern Atlantic basin. The nepheloid layer flows southward, following the pattern of
429 deep circulation (Fig. 7) and carrying IVML to the latitude of New Jersey at least (Deconinck
430 and Vanderaveroet, 1996).

431

432 **5. Conclusions**

433 (1) Most Heinrich events of the northwest Atlantic Ocean are characterized by major
434 modifications of the clay minerals association and incorporation of clay-size ice-rafted
435 particles to the sediments:

436 (a) Heinrich events H1, H2, H4, and H5 are enriched in illite, chlorite, and kaolinite.
437 Illite and chlorite are typically detrital clay minerals resulting from glacial erosion. In the

438 northwestern Atlantic basin, they mainly derive from the Precambrian and Paleozoic igneous
439 and sedimentary rocks of the North American continent (Piper and Slatt, 1977; Thiébault et
440 al., 1989). In the northwestern Atlantic basin, kaolinite is derived from adjacent landmasses
441 where it formed during pre-glacial or interglacial periods, and from old sedimentary
442 formations (such as the black Cretaceous mudstones of Labrador (Boyd and Piper, 1976;
443 Jennings, 1993).
444 (b) The Heinrich layers are also enriched in IVML, which formed during interglacial
445 periods through pedogenic processes (Berry and Johns, 1966). In the northwestern Atlantic
446 basin, these minerals have been transported by run-off during interglacial periods from the
447 Canadian Appalachian Mountains (Yang and Hesse, 1991) to the Labrador shelf (Fagel et al.,
448 1996).
449 (2) Clay mineral studies show that the Heinrich layers do not only result from an ice-
450 rafting mechanism, and the dynamic of their formation is complex and results from at least
451 two important mechanisms:
452 (a) Detrital carbonates and typically detrital clay minerals (illite C chlorite C kaolinite)
453 are carried and discharged by icebergs during disintegration of the Laurentide ice-sheet.
454 (b) The enhanced supply in IVML results from the erosion of the shelf during
455 formation of a dense nepheloid layer flowing at an intermediate water depth, and following
456 the general pattern of intermediate and deep-water circulation. Such a nepheloid layer is
457 seasonally documented in the modern Labrador Sea (Eittreim et al., 1969; Eittreim and
458 Ewing, 1974; Biscaye and Eittreim, 1974, 1977). Andrews and Tedesco (1992) first proposed
459 its contribution to the Heinrich deposits on the basis of high sedimentation rates. This
460 mechanism is more rapid, and at least as important as ice-rafting discharges, because of the
461 huge amounts of particles transported in a very short time. The extension of the nepheloid
462 layer is determined by comparison of mineralogical analyses of subsurface sediments from
463 different cores. The nepheloid layer forms in shallow areas and flows eastward along the
464 slope and in the basin at intermediate water depth, to the mid-oceanic ridge which prevents
465 penetration of the nepheloid layer into the northeastern Atlantic basin. The current flows
466 principally southward, following the main pattern of deep-water circulation.
467 (3) Comparison between the variations of IVML and of illite C chlorite C kaolinite,
468 indicates that increased mixed-layer supply by the nepheloid precedes the detrital clay supply
469 by ice-rafting processes. The nepheloid layer formation and ice-rafting processes do not
470 depend directly from each other. Nevertheless, ice-sheet dynamics are assumed to be
471 responsible for both mechanisms. This implies that ice-sheet dynamics are more complex than

previously thought, and that they strongly control the transport of fine particles to the ocean. Therefore, clay minerals could be used as markers for further investigations of the dynamics of ice-sheets.

Acknowledgements

We are grateful to Philippe Récourt for technical assistance. Review and constructive comments by C. Robert and K.T. Pickering are gratefully acknowledged. The coring cruise Paleocinat I of the French R/V *Le Suroît* was supported by Genavir and IFREMER. This work was financially supported by PNEDC from INSU, by the EEC program Environment and Climate (EV5V-CT92-0117) and by the URA 719 CNRS 'Sédimentologie et Géodynamique', Université de Lille 1.

References

Albarède, F., 1995. Introduction to Geochemical Modeling. Cambridge Univ. Press, 543 pp.

Andrews, J.T., Tedesco, K., 1992. Detrital carbonate-rich sediments, northwestern Labrador Sea — implications for ice sheet dynamics and icebergs rafting (Heinrich) events in the north Atlantic. Geology 20, 1087–1090.

Andrews, J.T., Erlenkeuser, H., Tedesco, K., Aksu, A.E., Jull, A.J.T., 1994. Late Quaternary (stage 2 and 3) meltwater and Heinrich events, northwest Labrador Sea. Quat. Res. 41, 26–34.

Andrews, J.T., Osterman, L.E., Jennings, A.E., Syvitski, J.P.M., Miller, G.H., Weiner, N., 1996. Abrupt changes in marine conditions, Sunneshine fiord, eastern Baffin Island, NWT, during the last deglacial transition: Younger Dryas and H-0 events. In: Andrews, J.T., Austin, W.E.N., Bergsten, H., Jennings, A.E. (Eds.), Late Quaternary Palaeoceanography of the North Atlantic Margins. Geol. Soc. Spec. Publ. 111, 11–27.

April, R.H., Hluchy, M.M., Newton, R.M., 1986. The nature of vermiculite in Adirondack soils and till. Clays Clay Miner. 34 (5), 549–556.

Berry, R.W., Johns, W., 1966. Mineralogy of the clay-size fractions of some north-Atlantic Arctic Ocean bottom current. Geol. Soc. Am. Bull. 77, 183–196.

Berthois, L., Latouche, C., Parra, M., 1973. Etude minéralogiques et géochimiques de quelques sédiments de la zone comprise entre les archipels Faeroes, Shetland, Orcades et Hébrides. Bull. Inst. Geol. Bassin Aquitaine 14, 3–17.

Biscaye, P., 1965. Mineralogy and sedimentation of recent deep-sea clay in the Atlantic Ocean and adjacent seas and oceans. Geol. Soc. Am. Bull. 76, 803–832.

Biscaye, P., Eittreim, S.L., 1974. Variations in benthic boundary layer phenomenon: nepheloid layer in the North American basin. In: Gibbs, R.J. (Ed.), Suspended Solids in Water. Plenum Press, New York, NY, pp. 227–260.

Biscaye, P., Eittreim, S.L., 1977. Suspended particulate loads and transports in the nepheloid layer of the abyssal Atlantic Ocean. Mar. Geol. 23, 155–172.

Bond, G., Heinrich, H., Broecker, W., Labeyrie, L., McManus, J., Andrews, J., Huon, S., Jantschick, R., Clasen, S., Simet, C., Tedesco, K., Klas, M., Bonami, G., Ivy, S., 1992. Evidence for massive discharges of icebergs into the North Atlantic Ocean during the last glacial period. Nature 360, 245–249.

Bout-Roumazeilles, V., 1995. Relations entre les variabilités minéralogiques et climatiques enregistrées dans les sédiments de l'Atlantique nord pendant les huit derniers stades glaciaires/interglaciaires. Thèse Univ. Lille I, 280 pp.

Boyd, R.W., Piper, D.J.W., 1976. Baffin Bay continental shelf clay mineralogy. Marit. Sediment. 12 (1), 17–18.

Broecker, W., Bond, G., Klas, M., Clark, E., McManus, J., 1992. Origin of the northern Atlantic's Heinrich events. Clim. Dyn. 6, 265–279.

Chamley, H., 1975. Remarque sur la sédimentation argileuse quaternaire en Mer de Norvege. Union Océanogr. Fr. 7, 15– 20.

Chamley, H., 1989. Clay Sedimentology. Springer, Berlin, 623 pp.

Cortijo, E., Reynaud, J.Y., Labeyrie, L., Paillard, D., Lehman, B., Cremer, M., Grousset, F., 1995. Etude de la variabilité climatique à haute résolution dans des sédiments de l'Atlantique Nord. C. R. Acad. Sci. Ser. II 321, 231–238.

Darby, S.A., 1975. Kaolinite and other clay minerals in Arctic Ocean sediments. J. Sediment. Petrol. 45, 272–279.

Deconinck, J.F., Vanderaveroet, P., 1996. Eocene to Pleistocene clay mineral sedimentation off New-Jersey, western north Atlantic (ODP Leg 150, sites 903 and 905). Proc. ODP Sci. Results 150, 147–170.

Desprairies, A., Bonnot-Courtois, C., 1980. Relation entre la composition des smectites d'alteration sous-marine et leur cortège de terres rares. Earth Planet. Sci. Lett. 48, 124–130.

Dickson, R.R., Brown, J., 1994. The production of North Atlantic Deep Water: sources, rates and pathways. J. Geophys. Res. 99, 12319–12341.

Eittreim, S.L., Ewing, M., 1974. Turbidity distribution in the deep waters of the western Atlantic trough. In: Gibbs, R.J. (Ed.), Suspended Solids in Water. Plenum Press, New York, NY, pp. 213–225.

Eittreim, S., Ewing, H., Thorndike, E.M., 1969. Suspended matter along the continental margin of the North American basin. Deep-Sea Res. 16, 613–624.

Elverhøi, A., 1979. Sedimentological and mineralogical investigations of quaternary bottom currents off the Norwegian West Coast. Nor. Geol. Tidsskr. 59, 273–284.

Fagel, N., Robert, C., Hillaire-Marcel, C., 1996. Clay mineral signature of the NW Atlantic Boundary Undercurrent. Mar. Geol. 130, 19–28.

Griffin, J.J., Windom, H., Goldberg, E.D., 1968. The distribution of clay minerals in the world ocean. Deep-Sea Res. 15, 433– 459.

Grousset, F., 1983. Sedimentogenèse d'un environnement de dorsale: la ride Açores-Islande au cours du dernier cycle climatique. Origines, vecteurs, flux des particules sédimentaires. Thèse Univ. Bordeaux, 232 pp.

Grousset, F., Chesselet, R., 1986. The Holocene sedimentary regime in the northern mid-Atlantic ridge region. Earth Planet. Sci. Lett. 78, 271–287.

Grousset, F.E., Labeyrie, L., Sinko, J.A., Cremer, M., Bond, G., Duprat, J., Cortijo, E., Huon, S., 1993. Patterns of ice-rafted detritus in the glacial north Atlantic (40º-55ºN). Palaeoceanography 8 (2), 175–192.

Heinrich, H., 1988. Origin and consequences of cyclic ice-rafting in the northeast Atlantic Ocean during the past 130,000 years. Quat. Res. 29, 142–152.

Holtzapffel, T., 1985. Les minéraux argileux. Préparation. Analyse diffractométrique et détermination. Mem. Soc. Geol. Nord, Lille 12, 136 pp.

Hulbe, C.L., 1997. An ice shelf mechanism for Heinrich layer production. Palaeoceanography 12 (5), 711–717.

Huon, S., Ruch, P., 1992. Mineralogical, K-Ar, and 86Sr/87Sr isotopes study of Holocene and late glacial sediment in a deep-sea core from northeast Atlantic Ocean. Mar. Geol. 107 (4), 275–282.

Jennings, A.E., 1993. The Quaternary history of Cumberland Sound, southeastern Baffin Island: the marine evidence. Géogr. Phys. Quat. 47, 21–42.

Jennings, A.E., Tedesco, K.A., Andrews, J.T., Kirby, M.E., 1996. Shelf erosion and glacial ice proximity in the Labrador Sea during and after Heinrich events (H-3 or 4 to H-0) as shown by foraminifera. In: Andrews, J.T., Austin, W.E.N., Bergsten, H., Jennings, A.E. (Eds.), Late Quaternary Palaeoceanography of the North Atlantic Margins. Geol. Soc. Spec. Publ. 111, 29–49.

Johnson, R.A., Wichern, D.W., 1982. Applied Multivariate Statistical Analysis. Prentice-Hall, Englewood Cliff, NY, 285 pp.

574 Kuhlemann, J., Lange, H., Paetsch, H., 1993. Implications of a connection between clay
575 mineral variations and coarse-grained debris and lithology in the central Norwegian-
576 Greenland Sea. Mar. Geol. 114, 1–11.
577 Lisitzin, A.P., 1972. Sedimentation in the world ocean. Soc. Econ. Paleontol. Mineral. Spec.
578 Publ. Tulsa, 218 pp.
579 Lucotte, M., Hillaire-Marcel, C., 1994. Identification des grandes masses d'eau dans les mers
580 du Labrador et d'Irminger. Can. J. Earth Sci. 31, 5–13.
581 MacAyeal, D.R., 1993. Binge/purge oscillations of the Laurentide ice sheet as a cause of the
582 North Atlantic's Heinrich events. Palaeoceanography 8 (6), 775–784.
583 Martinson, D.G., Pisias, N.G., Hays, J.D., Imbrie, J., Moore, T.C., Shackleton, N.J., 1987.
584 Age dating and the orbital theory of ice-ages: Development of high resolution 0 to 300 000-
585 year chronostratigraphy. Quat. Res. 27, 1–29.
586 McCartan, L., 1988. Mineralogy of the Haynesville, Virginia, cores. U.S. Geol. Surv. Prof.
587 Pap. 1489, B1–B9.
588 McCave, I.N., Tucholke, B.E., 1986. Deep current-controlled sedimentation in the western
589 North Atlantic. In: Vogt, P.R., Tucholke, B.E. (Eds.), The Geology of North America, Vol.
590 M, The Western North Atlantic Region. Geological Society of America, Boulder, CO, pp.
591 451–468.
592 Millot, G., 1970. Geology of Clays. Springer, Berlin, 425 pp.
593 Moyes, J., Duplessy, J.C., Gonthier, E., Latouche, C., Maillet, N., Parra, M., Pujol, C., 1964.
594 Les sédiments profonds actuels et pléistocène récent de l'Atlantique nord-oriental et du sud de
595 la Mer de Norvège. IIeme Colloque international sur l'exploitation des océans, Bordeaux, 4,
596 p. 201.
597 Naidu, A.S., Creager, J.S., Mowatt, T.C., 1982. Clay mineral dispersal patterns in the north
598 Bering and Chukchi Seas. Mar. Geol. 47, 1–5.
599 Nielsen, O.B., Cremer, M., Stein, R., Thiebault, F., Zimmerman, H., 1989. Analysis of
600 sedimentary facies, clay mineralogy, and geochemistry of the paleogene sediments of site
601 647, Labrador Sea . Proc. ODP Sci. Results 105, 101–110.
602 Paillard, D., Labeyrie, L., Yiou, P., 1996. Analyseries 1.0: a Macintosh software for the
603 analysis of geographical time-series. EOS 77, 379.
604 Parra, M., Delmont, P., Ferragne, A., Latouche, C., Puechmaille, C., 1985. Origin and
605 evolution of smectites in recent marine sediments of the NE Atlantic. Clay Miner. 20, 335–
606 345.

607 Petersen, L., Rasmussen, K., 1980. Mineralogical composition of the clay-size fraction of two
608 fluvio-glacial sediments from east Greenland. Clay Miner. 15, 135–145.
609 Piper, D.J.W., Slatt, R.M., 1977. Late Quaternary clay mineral distribution along the eastern
610 margin of Canada. Geol. Soc. Am. Bull. 86, 267–272.
611 Rateev, M.A., Gorbunova, Z.N., Lisitzin, A.P., Nasov, G.L., 1969. The distribution of the
612 clay minerals in the oceans. Sedimentology 13, 21–43.
613 Rich, C.I., 1956. Muscovite weathering in a soil developed in the Virginia Piedmont. Clays
614 Clay Miner. 16, 15–36.
615 Ruddiman, W.F., 1977. Late Quaternary deposition of ice-rafted sand in the sub-polar north
616 Atlantic (lat. 40º to 65ºN). Geol. Soc. Am. Bull. 88, 1813–1827.
617 Sancetta, C., Heusser, L., Labeyrie, L., Naidu, A.S., Robinson, S.W., 1985. Wisconsin-
618 Holocene paleoenvironment of the Bering Sea: evidence from diatoms, pollen, oxygen
619 isotopes and clay minerals. Mar. Geol. 62, 55–68.
620 Thiébault, F., Cremer, M., Debrabant, P., Foulon, J., Nielsen, O.B., Zimmerman, H., 1989.
621 Analysis of sedimentary facies, clay mineralogy, and geochemistry of the Neogene-
622 Quaternary sediments in site 645, Baffin Bay. Proc. ODP Sci. Results 105, 83–100.
623 Yang, C., Hesse, R., 1991. Clay minerals as indicators of diagenetic and anchimetamorphic
624 grade in an overthurst belt, external domain of southern Canadian Appalachians. Clay Miner.
625 26, 211–231.
626

627 **Figure captions**

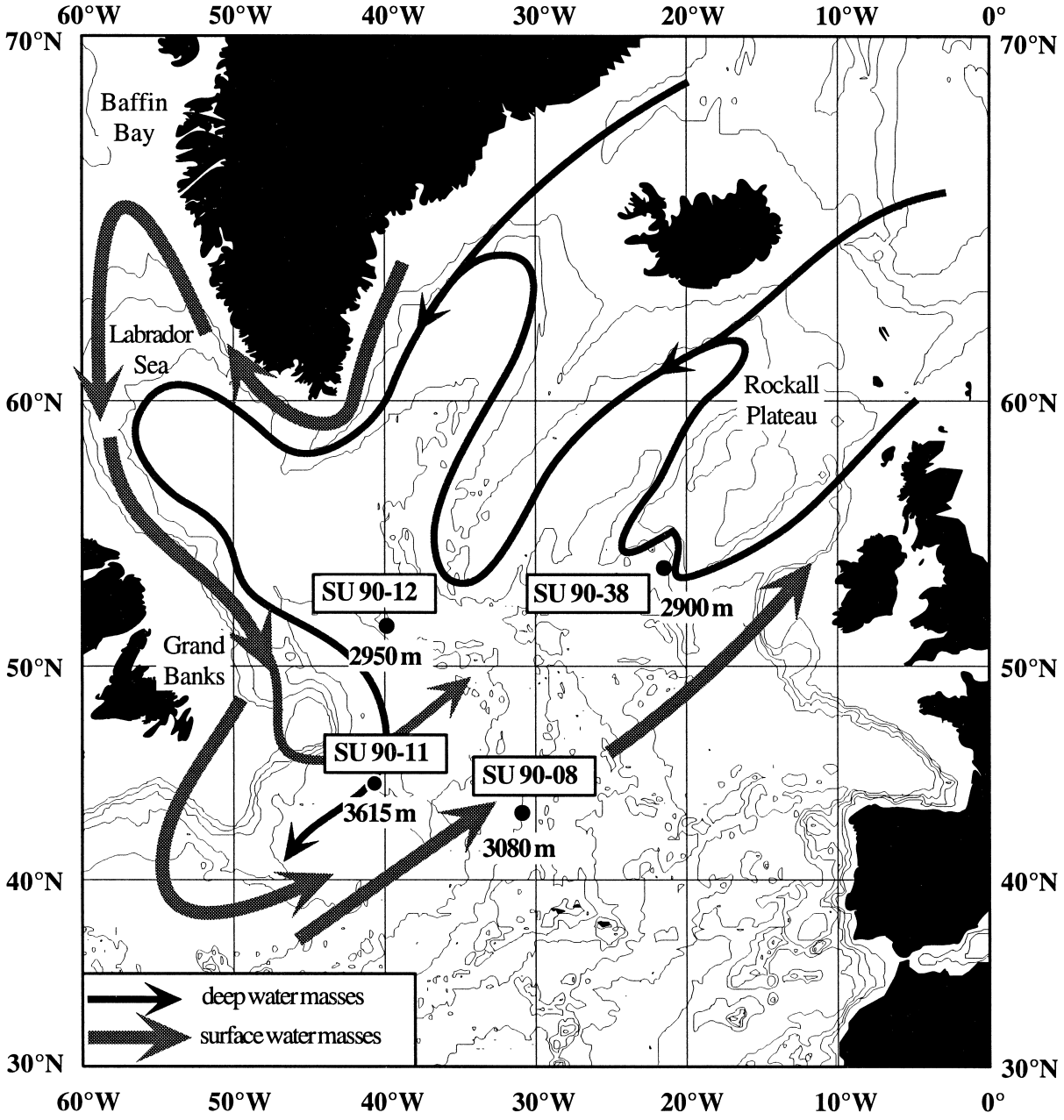

628

629 Fig. 1. Study area, cores location and main deep and surface circulation patterns modified
630 from McCave and Tucholke (1986), Dickson and Brown (1994) and Lucotte and Hillaire-
631 Marcel (1994).

632

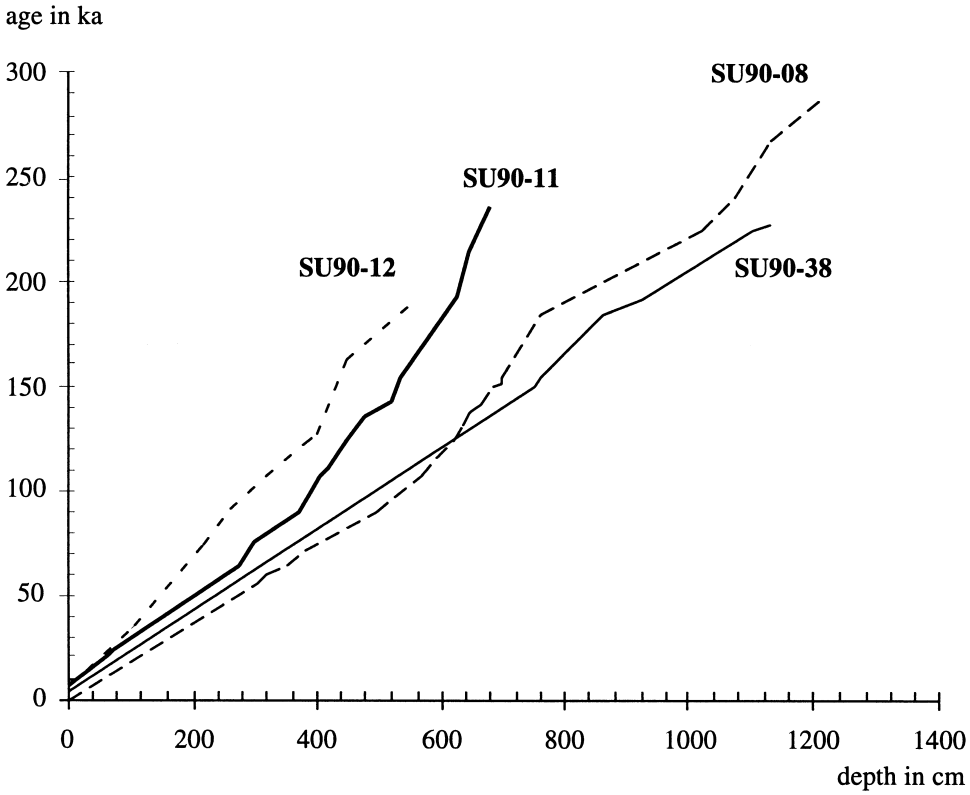

633

634 Fig. 2. Age–depth relation for the studied cores.

635

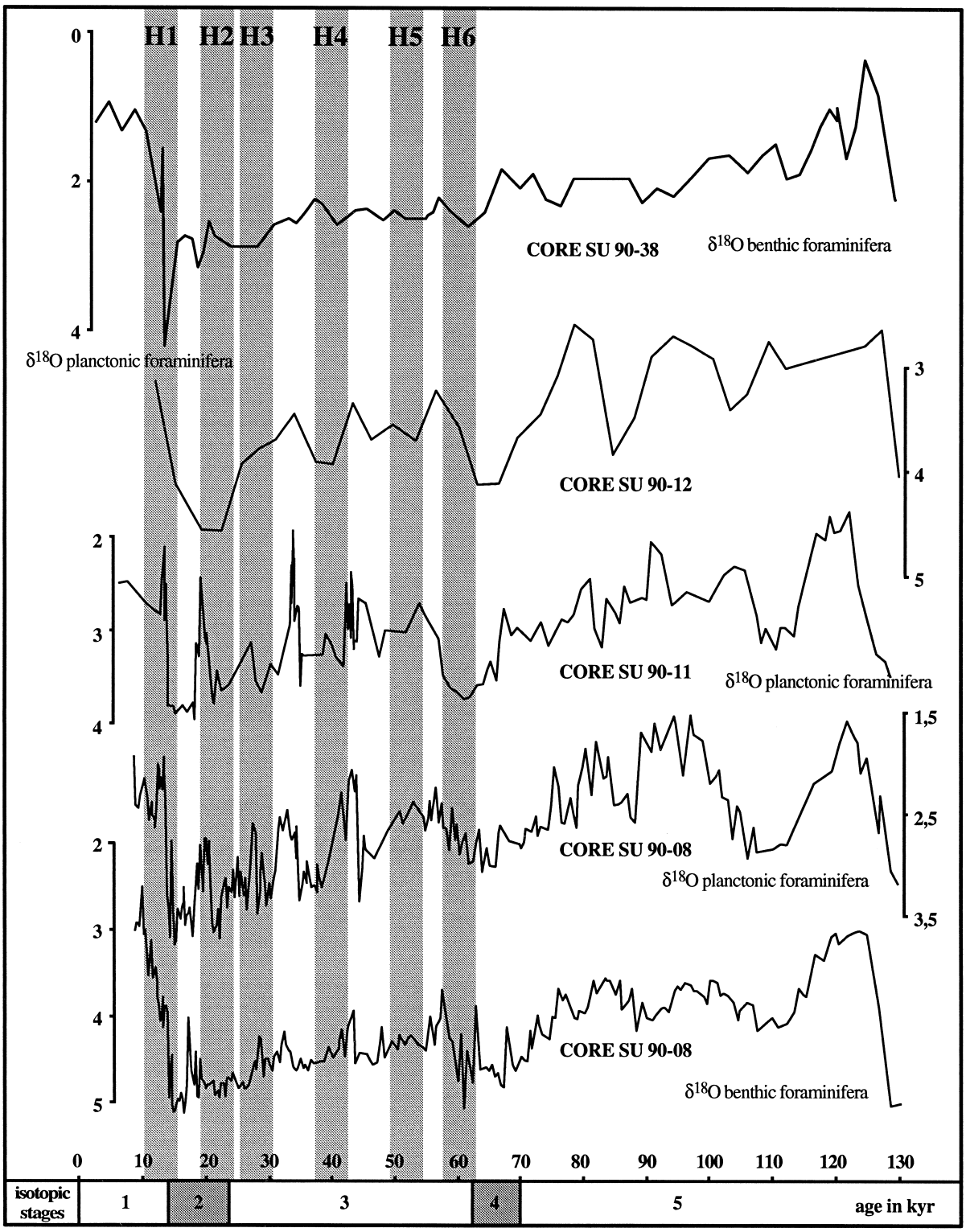

Fig. 3. $\delta^{18}O$ on benthic and planktonic foraminifera of cores SU90-08, SU90-11, SU90-12 and SU90-38. The Heinrich layers are indicated by gray rectangles.

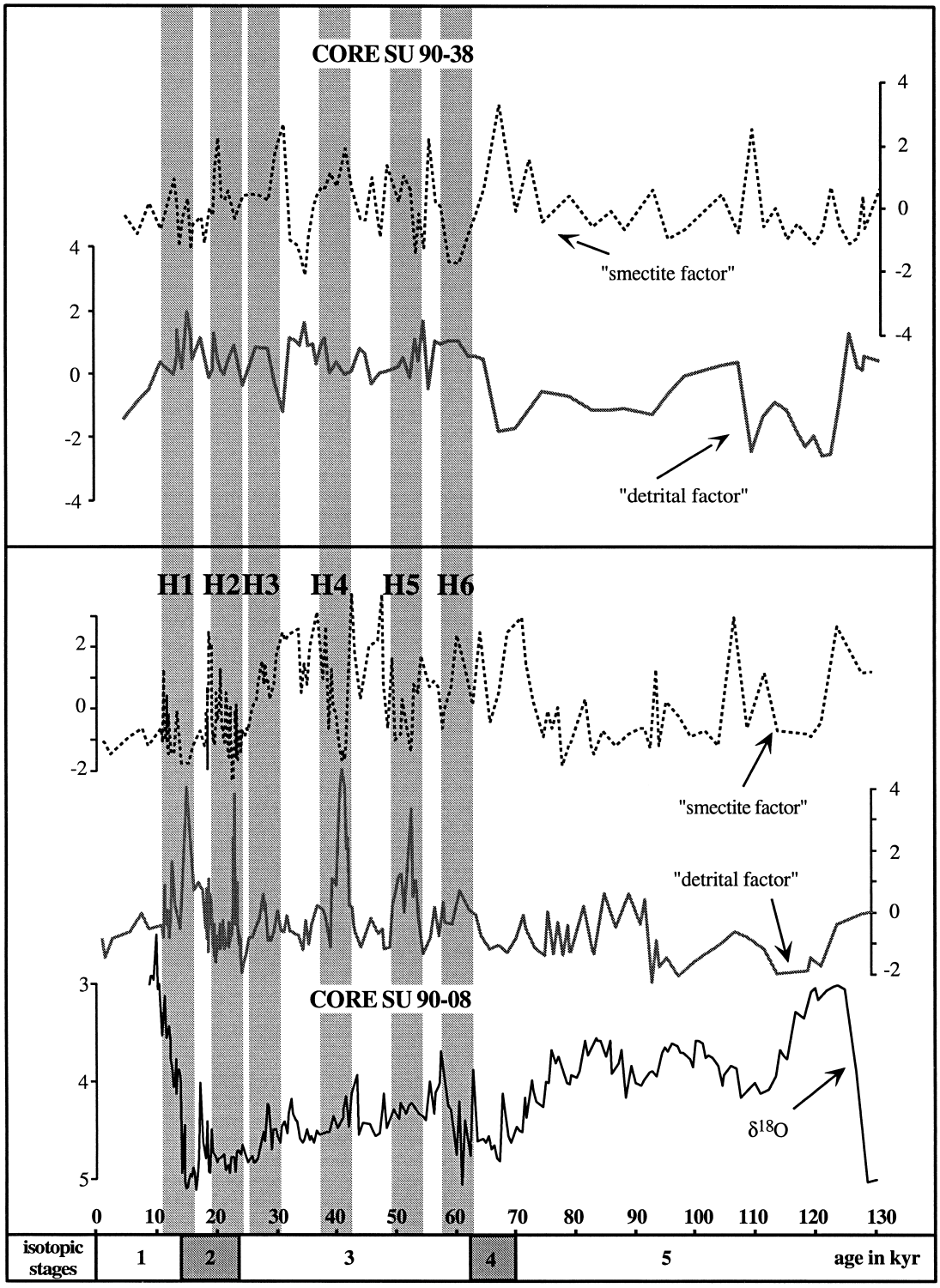

Fig. 4. Variations of the detrital (gray line) and smectite factors (dashed line), and $\delta^{18}O$ on benthic foraminifera over the last 130 kyr for cores SU90-08 (lower). Variations of the detrital and smectite factors over the last 130 kyr for core SU90-38 (upper). Heinrich Events *H1* to *H6* are indicated by gray rectangles.

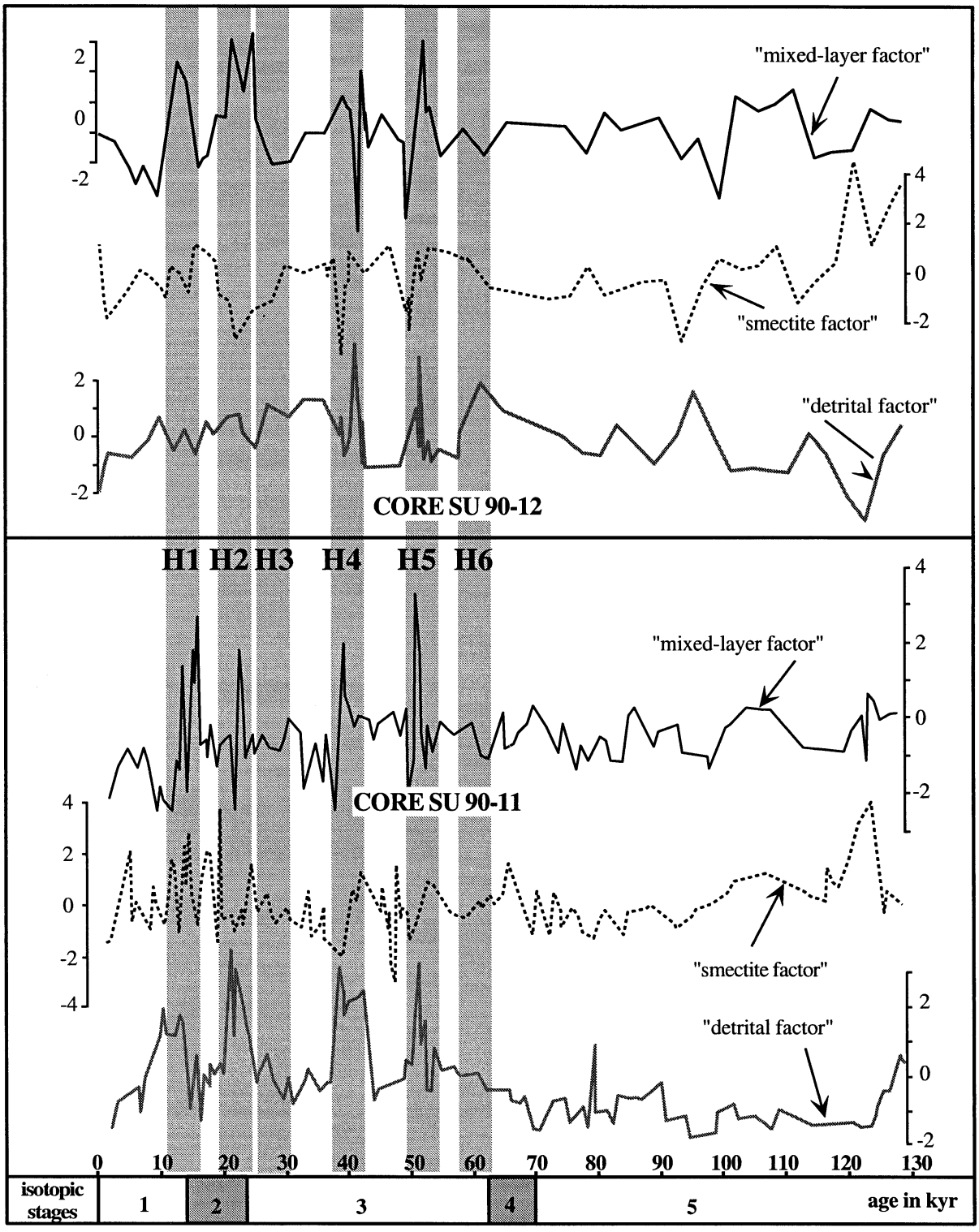

Fig. 5. Variations of the detrital (gray line), smectite (dashed line), and mixed-layer (solid line) over the last 130 kyr for cores SU90-11 (lower) and SU90-12 (upper). Heinrich Events *H1* to *H6* are indicated by gray rectangles.

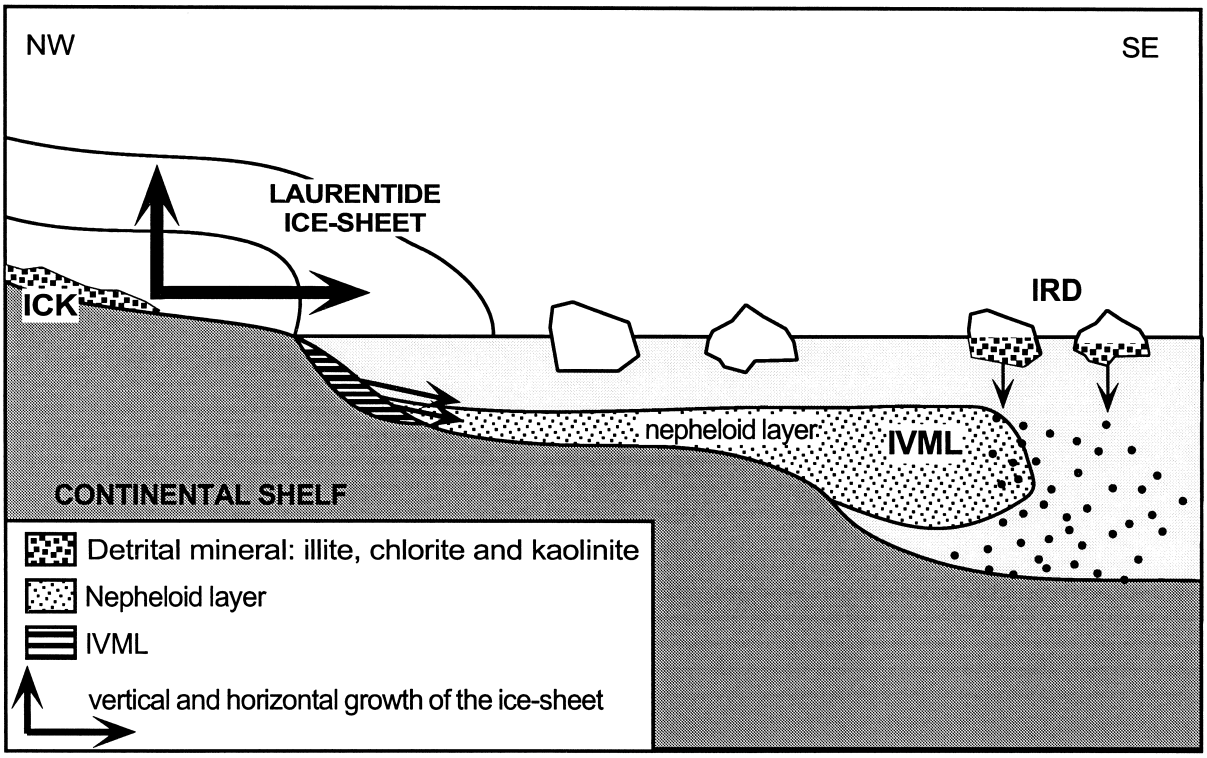

651

652 Fig. 6. Nepheloid layer and Ice-Rafted-Detritus transportation mechanisms since the Labrador
653 continental shelf area toward the open ocean during the Heinrich events, in relation with the
654 vertical and horizontal growth of the Laurentide ice-sheet. *ICK* = detrital minerals: illite,
655 chlorite, and kaolinite. *IVML* = illite-vermiculite mixed-layer red clay.

656

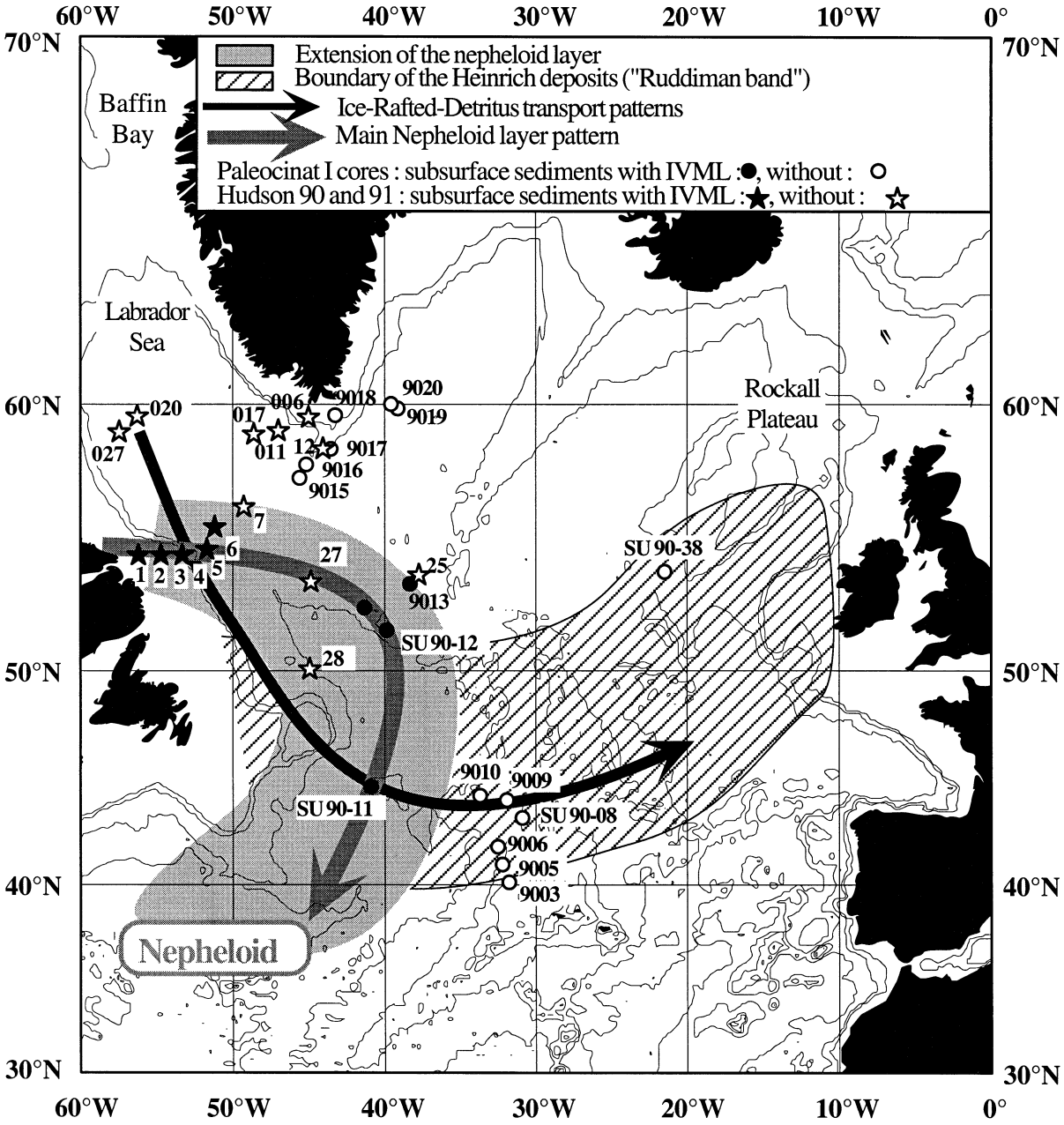

Fig. 7. Main sub-actual extension of the nepheloid layer main surface and IRD transportation patterns according to clay mineral analyses from Paleocinat I cores 9003 to 9020 (Bout-Roumazeilles, 1995) and from Hudson 90–91 cores (Fagel et al., 1996).

Table 1

Core characteristics

Cores	Latitude (N)	Longitude (W)	Depth (mbsf)	Length (m)
SU90-08	43°41′2	30°24′5	3080	12.27
SU90-11	44°43′6	40°15′8	3645	6.97
SU90-12	51°52′6	39°04′9	2950	15.5
SU90-38	54°05′4	21°04′9	2900	11.42

Table 2

Age–depth relation for the studied cores

SU90-08		SU90-11		SU90-12		SU90-38	
depth (cm)	age (ka)	depth (cm)	age (ka)	depth (cm)	age (ka)	depth (cm)	age (ka)
0	0	2.5	6	29.5	11.4	0	4.1
302	54.8	63	22	104	33.2	750	150.4
320	57.6	75	24	109	35.6	760	152.3
352	64.1	273	65	220.5	73.2	860	183.4
383	71.1	300	75	258.5	90.9	920	191.4
497	90.1	370	90	319.5	107.5	1100	225.2
526	96.4	404	107	380	122.2	1130	228.3
569.5	107.6	417.5	112	398.5	126.6		
589.5	115.9	445	125	448	162.8		
620	125	480	135	547.5	188.3		
633.5	131.1	520	143				
644.5	136.6	534	155				
653	139	624.5	193				
667	141.3	642.5	215				
685	149.3	677	237				
698.5	152.1						
699	152.6						
759	183.4						
1019	225.2						
1071	240.2						
1130	267.5						
1210	288.5						

669 Table 3

670 Mean clay mineral composition (%) and standard deviation (Sd) of sediments from the
671 studied cores without Heinrich layers data

Clay minerals	SU90-08		SU90-11		SU90-12		SU90-38	
	average	Sd	average	Sd	average	Sd	average	Sd
Chlorite	14	±3	20	±4	21	±4	14	±3
Illite	37	±7	34	±4	34	±5	39	±7
10-14s	6	±2	Tr.	–	–	–	–	–
10-14v	–	–	17	±7	18	±8	–	–
Smectite	33	±11	16	±7	15	±8	35	±11
Kaolinite	11	±3	12	±2	12	±2	11	±2
∑(I + C + K)	62		66		67		64	

10-14s = illite-smectite mixed-layer minerals; 10-14v = illite-vermiculite mixed-layer minerals.

672

673

674 Table 4

675 Mean clay mineral composition (%) and standard deviation (Sd) of Heinrich layers sediments
676 from the studied cores

Clay minerals	SU90-08		SU90-11		SU90-12		SU90-38	
	average	Sd	average	Sd	average	Sd	average	Sd
Chlorite	20	±2	20	±2	19	±2	14	±2
Illite	55	±6	40	±4	42	±5	42	±5
10-14s	–	–	–	–	–	–	–	–
10-14v	–	–	28	±8	32	±11	–	–
Smectite	10	±2	–	–	8	±2	32	±4
Kaolinite	15	±2	12	±4	11	±3	12	±3
∑(I + C + K)	90		72		60		68	

10-14s = illite-smectite mixed-layer minerals; 10-14v = illite-vermiculite mixed-layer minerals.

677
678

679 Table 5

680 Correlation matrix between clay minerals species for the studied cores

Cores	Clay minerals	Chlorite	Illite	10-14v	Smectite	Kaolinite
SU90-08	chlorite	1				
	illite	0.8	1			
	smectite	0.0	−0.0		1	
	kaolinite	0.8	0.7		0.0	1
SU90-11	chlorite	1				
	illite	0.8	1			
	10-14v	−0.0	−0.0	1		
	smectite	0.1	0.3	−0.6	1	
	kaolinite	0.8	0.8	−0.2	0.4	1
SU90-12	chlorite	1				
	illite	0.8	1			
	10-14v	−0.0	−0.1	1		
	smectite	0.5	0.5	−0.5	1	
	kaolinite	0.7	0.8	−0.0	0.5	1
SU90-38	chlorite	1				
	illite	0.9	1			
	smectite	0.3	0.4		1	
	kaolinite	0.8	0.8		0.2	1

681 10-14v = illite-vermiculite mixed-layer minerals.

682

683 Table 6

684 Scores of the orthogonal transformation varimax solution (factor analysis) for the detrital,

685 smectite, and mixed-layer factors for the studied cores

Cores	Clay minerals	Detrital factor	Smectite factor	Mixed-layer factor
SU90-08	chlorite	0.9	0.0	
	illite	0.9	−0.0	
	smectite	0.0	1	
	kaolinite	0.9	0.0	
SU90-11	chlorite	0.9	−0.1	−0.0
	illite	0.9	0.1	0.0
	10-14v	−0.0	−0.3	0.9
	smectite	0.1	0.9	−0.3
	kaolinite	0.9	0.3	−0.0
SU90-12	chlorite	0.9	0.0	0.0
	illite	0.9	0.1	−0.0
	10-14v	−0.0	−0.1	1
	smectite	0.4	0.8	−0.3
	kaolinite	0.8	0.3	0.0
SU90-38	chlorite	0.9	0.1	
	illite	0.9	0.2	
	smectite	0.1	1	
	kaolinite	0.9	0.0	

686 10-14v = illite-vermiculite mixed-layer minerals.

687

688 Table 7

689 Core characteristics, and 10-14v percentages in subsurface sediments

Cores	Lat. (N)	Long (W)	Depth (mbsf)	% 10-14v
9009	31°44′9	31°44′9	3370	–
9003	40°30′3	32°03′2	2475	–
9005	41°38′4	32°15′4	3285	–
9006	42°01′8	32°42′7	3510	–
SU90-08	43°31′2	30°24′5	3080	–
9010	44°42′1	34°42′3	3965	–
SU90-11	44°43′6	40°15′8	3645	26
28[a]	50°12′2	45°41′1	3448	–
SU90-12	51°52′6	39°47′4	2950	20
9013	52°52′4	41°15′7	3660	5
27[a]	53°19′7	45°15′6	3378	–
25[a]	53°58′5	38°38′2	3603	–
2[a]	54°44′5	55°35′0	301	35
3[a]	54°49′2	53°43′9	340	27/tr
1[a]	54°52′9	56°26′9	530	12
4[a]	54°54′0	52°52′0	1364	5
5[a]	55°02′0	52°44′7	1984	tr.
6[a]	52°07′7	52°07′7	2648	tr.
7[a]	56°36′9	49°45′0	3992	–
9014	57°39′2	46°51′2	2924	5
9015	57°58′5	45°54′8	2420	–
017[a]	58°12′5	48°21′6	3379	–
9016	58°13′2	45°10′5	2100	–
020[a]	58°21′5	57°27′3	2865	–
12[a]	58°42′8	53°57′0	1559	–
027[a]	58°45′7	57°05′1	3032	–
9017	58°47′8	43°57′0	1605	–
011[a]	58°54′8	47°05′1	2805	–
9018	59°22′1	43°27′0	1015	–
006[a]	59°29′4	45°52′2	1105	–
9019	59°32′2	39°27′8	2925	–
9020	59°51′7	39°39′8	2700	–

Cores 9003 to 9020 from Paleocinat I cruise (Bout-Roumazeilles, 1995).

[a] Cores from Hudson 90–91 cruises (Fagel et al., 1996).

690